Search for Direct Pair Production of Top Squark in the Final State of Two Tau Leptons at ATLAS

AHMED HASIB

Homer L. Dodge Department of Physics and Astronomy, University of Oklahoma, Norman, Oklahoma, USA

On behalf of the ATLAS Collaboration

Abstract. The first hadron collider search for direct pair production of the supersymmetric partner of the top quark, decaying via a scalar tau to a nearly massless gravitino is performed using data from proton–proton collisions at the Large Hadron Collider. The collision data collected by the ATLAS detector corresponding to an integrated luminosity of 20 fb^{-1} at the center-of-mass energy of 8 TeV are used for these results. Top squark candidates are searched for in events with either two hadronically decaying tau leptons, one hadronically decaying tau and one light lepton, or two light leptons. No significant excess over the Standard Model expectation is observed. Exclusion limits at 95% confidence level are set as a function of the top squark and scalar tau masses. Depending on the scalar tau mass, ranging from the 87 GeV LEP limit to the top squark mass, lower limits between 490 GeV and 650 GeV are placed on the top squark mass within the model considered.

1 INTRODUCTION

Supersymmetry (SUSY), a possible extension of the SM, can naturally resolve the hierarchy problem of the Standard Model (SM) by introducing a supersymmetric partner of the top quark [1]. The supersymmetric top quark partner with a mass close to the electroweak symmetry breaking energy, would stabilize the Higgs boson mass against the quadratically divergent quantum corrections and can be discovered at the Large Hadron Collider (LHC) [2]. In a minimal supersymmetric extension of the SM, the scalar partners of the left-handed and right-handed quarks and leptons mix, to form two top squark and two slepton mass eigenstates, respectively. The lighter of the two squark and stau particles is referred to as scalar top ($\tilde{t}_1$) and scalar tau ($\tilde{\tau}_1$), respectively. The decay processes of the SUSY particles are largely dependent on the SUSY symmetry breaking scenario under consideration. In the case of gauge mediated supersymmetry breaking, the lightest supersymmetric particle is a gravitino ($\tilde{G}$). In such a scenario, a complex three-body decay of $\tilde{t}_1$ to $b\nu_\tau\tilde{\tau}_1$ can be dominant, where ν_τ is the tau neutrino, followed by the scalar tau decay into tau lepton and a gravitino.
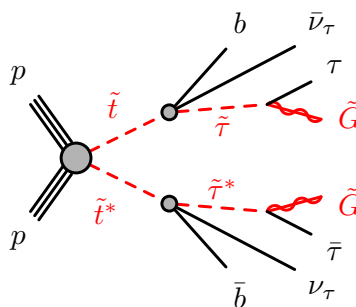

FIGURE 1. Diagram showing the decay topology of the signal process. Taken from Reference [3].

This paper presents a dedicated search for pair production of scalar tops in a final state with two tau leptons, two

jets initiated from *b*-quarks (*b*-jets), and two very light gravitationally interacting particles. The decay topology of the signal process is shown in Figure 1. The model considered is a simplified model in which all the supersymmetric particles other than the scalar top and the ones entering its decay chain are decoupled. In order to maximize the sensitivity, two distinct analyses are performed based on the decay mode of the tau leptons in the final state: one analysis requires two hadronically decaying tau leptons (the hadron–hadron channel) and the other requires one hadronically decaying tau lepton and one tau decaying into an electron or muon, plus neutrinos (the lepton–hadron channel). In addition, the results of the search reported in Reference [4], sensitive to events where both tau leptons decay leptonically (lepton–lepton channel), are reinterpreted and limits are set on the scalar top and scalar tau masses.

2   THE ATLAS DETECTOR

The ATLAS detector [5] is the largest particle detector at the LHC measuring 45m in length and 25m in diameter. It is a multipurpose detector with forward-backward cylindrical symmetry and divided into four main subsystems. The inner detector (ID) covers the pseudorapidity [1] range, $|\eta| < 2.5$ and consists of a silicon pixel detector, a semiconductor microstrip detector, and a transition radiation tracker. The ID is surrounded by a 2T solenoidal superconducting magnet which allows for precision tracking of charged particles and vertex reconstruction. The electromagnetic sampling calorimeter uses liquid-argon as the sampling material covering $|\eta| < 3.2$. A scintillator-tile calorimeter provides energy measurements for the hadrons within $|\eta| < 1.7$. The muon spectrometer is the outermost subsystem, consisting of three air-core superconducting toroidal magnets, each with eight superconducting coils, tracking chambers (covering $|\eta| < 2.7$) and trigger chambers (covering $|\eta| < 2.4$).

3   SIGNAL SELECTION AND BACKGROUND ESTIMATION

The data sample used in this paper was recorded in 2012, with the LHC operating at the center of mass energy $\sqrt{s} = 8$ TeV. The data are collected based on the decisions of a three-level trigger system [6]. Events are selected for the electron–hadron (muon–hadron) channel if they are accepted by a single-electron (single-muon) trigger. For the hadron–hadron channel, a missing transverse momentum ($\mathbf{p}_T^{\text{miss}}$) trigger is used. After beam, detector and data-quality requirements, the integrated luminosity of the data samples in the hadron–hadron and lepton–hadron channels are 20.1 fb^{-1}and 20.3 fb^{-1}, respectively. A number of simulated event samples are also used to model the signal and describe the background processes.

The analysis is based on cut and count method to estimate the signal and background contributions and relies on the following discriminating variables to differentiate the signal from the SM backgrounds:

- The transverse mass associated with two final-state objects *a* and *b*, defined as,

$$m_T (\text{a, b}) = \sqrt{m_a^2 + m_b^2 + 2\left(E_T^a E_T^b - \mathbf{p}_T^a \cdot \mathbf{p}_T^b\right)}, \tag{1}$$

  where m, E_T and $\mathbf{p}_T$ are the object mass, transverse energy and transverse momentum vector, respectively.
- The *stransverse mass* (m_{T2}) [7, 8] computed as,

$$m_{T2} (\text{a, b}) = \sqrt{\min_{\mathbf{q}_T^a + \mathbf{q}_T^b = \mathbf{p}_T^{\text{miss}}} \left(\max\left[m_T^2\left(\mathbf{p}_T^a, \mathbf{q}_T^a\right), m_T^2\left(\mathbf{p}_T^b, \mathbf{q}_T^b\right)\right]\right)}, \tag{2}$$

  where $\mathbf{q}_T^a$ and $\mathbf{q}_T^b$ are vectors satisfying $\mathbf{q}_T^a + \mathbf{q}_T^b = \mathbf{p}_T^{\text{miss}}$, and the minimum is taken over all possible choices of $\mathbf{q}_T^a$ and $\mathbf{q}_T^b$.

The selection criteria on these variables are different for the hadron–hadron and the lepton–hadron channels.

---

[1] ATLAS uses a right-handed coordinate system with its origin at the nominal interaction point (IP) in the centre of the detector and the *z*-axis along the beam pipe. The *x*-axis points from the IP to the centre of the LHC ring, and the *y*-axis points upward. Cylindrical coordinates (r, ϕ) are used in the transverse plane, ϕ being the azimuthal angle around the *z*-axis. The pseudorapidity is defined in terms of the polar angle θ as $\eta = -\ln\tan(\theta/2)$.

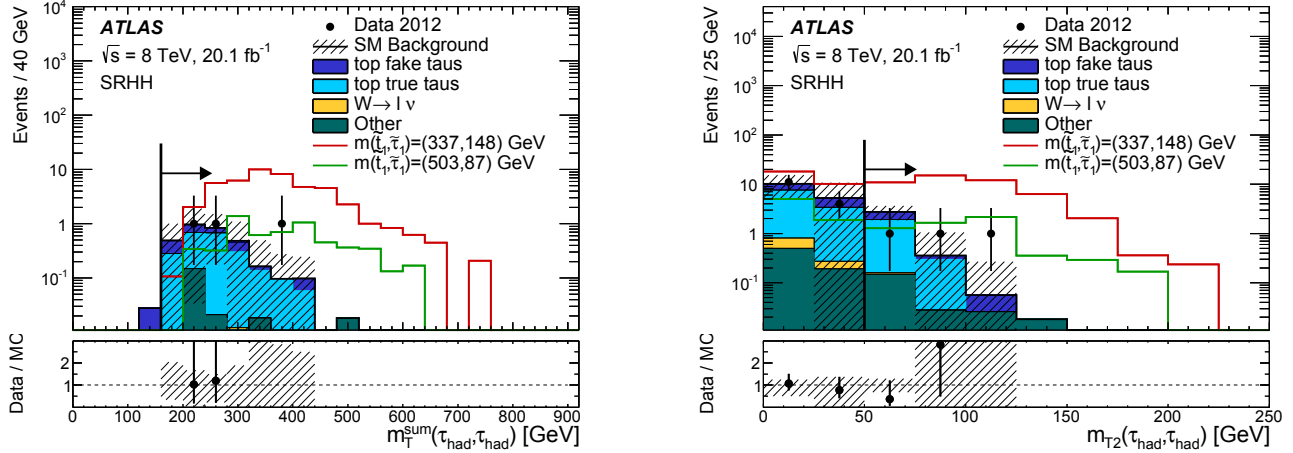**FIGURE 2.** Left: distribution of $m_T^{sum}(\tau_{had}, \tau_{had})$ for the events passing all the hadron–hadron signal region requirements, except that on $m_T^{sum}(\tau_{had}, \tau_{had})$. Right: distribution of $m_{T2}(\tau_{had}, \tau_{had})$ for the events passing all the hadron–hadron signal region requirements, except that on $m_{T2}(\tau_{had}, \tau_{had})$. The contributions from all SM backgrounds are shown as a histogram stack; the bands represent the total uncertainty. The background yields have been rescaled by the post-fit normalisation factors. The arrows mark the cut values used to define the SRs. The distributions expected for two signal models are also shown. Taken from Reference [3].

3.1 Hadron–hadron channel

The events in the hadron–hadron channel are required to have exactly two opposite-charged hadronically decaying tau leptons (τ_{had}), no electrons or muons, and at least two jets, and at least one of which is initiated by a b-quark. In addition, the following discriminating variables are used to define the signal region:

- m_{T2} (τ_{had}, τ_{had}) of the hadronically decaying taus and the missing transverse momentum as defined in Equation 2. This variable is bounded from above by the W boson mass and differentiates the dominant $t\bar{t}$ background, where the taus originate from W bosons, from the signal processes.
- m_T^{sum} (τ_{had}, τ_{had}), the sum of the transverse mass of each τ_{had} candidate and missing transverse momentum as defined in Equation 1.

Figure 2 shows distributions of these two variables and the requirement applied to construct the signal region (SR) of the hadron–hadron channel along with the expected backgrounds. The signal efficiency, defined as the total number of signal events that pass the full selection over the total number of generated events, is weakly dependent on the scalar tau mass and increases from 0.02% to 0.7% as the scalar top mass increases from 150 GeV to 700 GeV, for a scalar tau mass of 87 GeV.

The background contributions in this SR can be grouped into three categories. In the first category of backgrounds, both the final state hadronically decaying tau leptons are real. It consists of mainly $t\bar{t}$ events, with smaller contributions from single-top quark, Z+jets, diboson (WW, WZ, ZZ) and $t\bar{t} + V(= W, Z)$ production. These type of backgrounds are estimated directly in the simulation. Events where an electron or a jet is misidentified as a τ_{had} (*fake*-τ_{had}) is the second category of backgrounds. Backgrounds of this type are composed of $t\bar{t}$, single-top and W+jets events. The single-fake τ_{had} backgrounds are estimated in dedicated regions of phase space, called control region (CR), where the signal events do not contribute. A simultaneous likelihood fit is performed to determine the normalization factors of these backgrounds constrained to the number of data events in each CR, with the systematic uncertainties discussed in Section 4 as nuisance parameters. The last category of backgrounds with contributions smaller than 4.5%, are composed of two-fake τ_{had} and they are estimated using simulation without normalizing to data in a CR.

3.2 Lepton–hadron channel

The lepton–hadron search channel targets both low-mass and high-mass scalar top quarks. This selection requires exactly one hadronically decaying tau, exactly one electron or muon, where the hadronically decaying tau and the
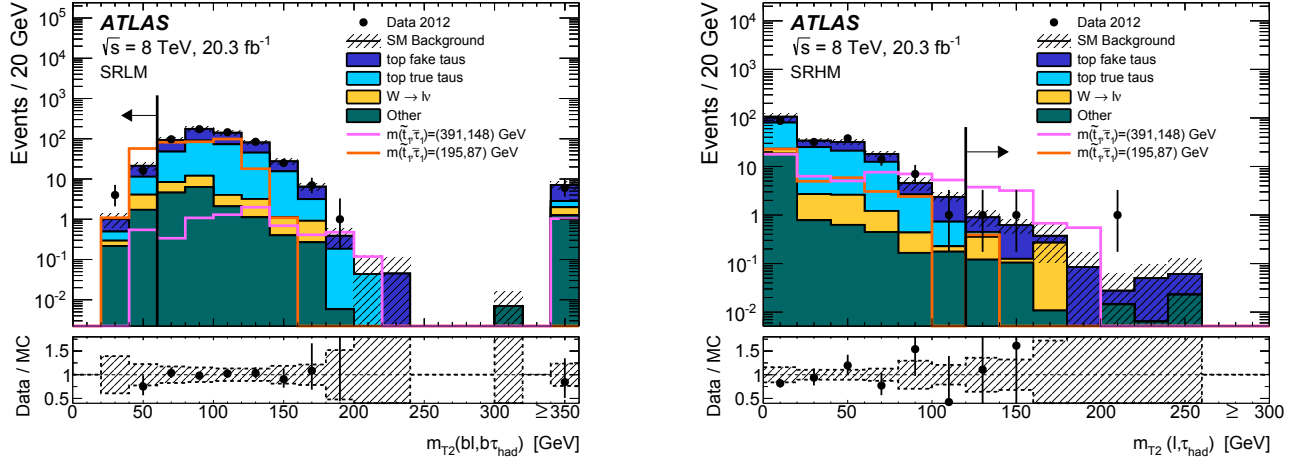
FIGURE 3. Left: distribution of $m_{T2}(b\ell, b\tau_{had})$ for events passing all the lepton–hadron LM signal region requirements, except that on $m_{T2}(b\ell, b\tau_{had})$. Right: distribution of $m_{T2}(\ell, \tau_{had})$ for events passing all the lepton–hadron HM signal region requirements, except that on $m_{T2}(\ell, \tau_{had})$. The contributions from all SM backgrounds are shown as a histogram stack; the bands represent the total uncertainty. The background yields have been rescaled by the post-fit normalisation factors. The arrows mark the cut values used to define the SRs. The overflow bin in the $m_{T2}(b\ell, b\tau_{had})$ plot is filled with the events that have for both pairings of $m(b\ell)$ and $m(b\tau_{had})$ at least one invariant mass larger than m_t. The distributions expected for two signal models are also shown. Taken from Reference [3].

lepton have opposite electric charge. Each event is also required to contain at least two jets, where at least one (high-mass) or two (low-mass) of the jets are originated from a b-quark. In addition, the following discriminating variables are used:

- $m_{T2}(\ell, \tau_{had})$, calculated using the momenta of the light lepton and the τ_{had}. This variable is bounded from above by the W boson mass. The $t\bar{t}$ and Wt processes where the light lepton, τ_{had} and missing transverse momentum originate from a W boson can be distinguished with this variable. The high-mass selection requires this variable to be large, because its distribution for signal models with heavy scalar taus and scalar top, peaks at higher values than for the top-quark-dominated SM background.
- $m_{T2}(b\ell, b\tau_{had})$, calculated using two jets originated from a b-quark. For $t\bar{t}$ events where the jet and the lepton belong to the decay of the same top quark, this variable is bounded from above by the top-quark mass. Whereas, for the signal events, the upper bound on this variable is the scalar top mass. A maximum cut value is therefore used for the low-mass selection.

The distributions for these variables for the low mass and the high mass points are shown in Figure 3 along with the expected background contributions. The signal selection efficiency of the low mass selection is between 0.008% and 0.01% for the models with scalar top mass between 150 GeVand 200 GeV, while for high mass selection it varies between 0.0007% and 1% for a scalar top mass between 200 GeVand 700 GeV.

The background contribution in the lepton–hadron signal region can be grouped into two categories. The first type of background is dominated by W+jets processes where the light lepton is always a real lepton from W decay, while the τ_{had} is faked by a recoiling hadronic object. The second category is contributed by $t\bar{t}$ and Wt processes where the light lepton is originated from the W boson and the τ_{had} can be either real or fake. Dedicated CRs are used to estimate these backgrounds. A simultaneous likelihood fit is performed to obtain the normalization factors for each background, using the observed number of data events as a constraint, along with the systematic uncertainties as nuisance parameters.

4   SYSTEMATIC UNCERTAINTIES

Various sources of systematic uncertainties originated from detector simulation and modeling of the major SM backgrounds, affecting the predicted background yields in the SRs, are taken into account. The uncertainties are either

computed directly in the SR where are the backgrounds are estimated from simulation, or propagated through the fit for backgrounds that are normalized in CRs. The impact of systematic uncertainties on the total background estimated in the different SRs is shown in Table 1, quoting the relative background uncertainty attributed to each source.

TABLE 1. Summary of background estimates and the associated total uncertainties. The size of each systematic uncertainty is quoted as a relative uncertainty on the total background. A dash indicates a negligible contribution to the uncertainty. The individual uncertainties can be correlated, and thus do not necessarily sum in quadrature to the total relative uncertainty. The observed number of events in each signal region is also shown. Taken from Reference [3].

	hadron–hadron	lepton–hadron (low-mass)	lepton–hadron (high-mass)
Observed events	3	20	3
Background events	3.1 ± 1.2	22.1 ± 4.7	2.1 ± 1.5
Uncertainty Breakdown [%]:			
Jet energy scale and resolution	17	13	2
Tau energy scale	9	4	3
Cluster energy scale and resolution	1	2	4
b-tagging	2	4	2
Top-quark theory uncertainty	37	11	64
W+jets theory and normalisation	-	1	19
Simulation statistics	20	6	21
Top normalisation	18	6	20

5   RESULTS AND INTERPRETATION

Good agreement is seen between the observed yields and the background estimates. Upper limits at 95% confidence level (CL) on the number of beyond-the-SM (BSM) events for each signal region are derived with the CL_s likelihood ratio prescription as described in Reference [9]. The limits are calculated for each signal region separately, with the observed number of events, the expected background and the background uncertainty as input to the calculation. Dividing the limits on the number of BSM events by the integrated luminosity of the data sample, these can be interpreted as upper limits on the visible BSM cross section, $\sigma_{\mathrm{vis}} = \sigma \times \mathcal{A} \times \epsilon$, where σ is the production cross section for the BSM signal, $\mathcal{A}$ is the acceptance defined as the fraction of events passing the geometric and kinematic selections at particle level, and ϵ is the detector reconstruction, identification and trigger efficiency. These quantities are summarized in Table 2.

TABLE 2. Left to right: Total constrained background yields, number of observed events, 95% CL observed (expected) upper limits on the number of BSM events, $S^{95}_{\mathrm{obs.(exp.)}}$, and the visible cross section, $\langle \mathcal{A}\epsilon\sigma \rangle^{95}_{\mathrm{obs.(exp.)}}$. Taken from Reference [3].

Signal Region	Background	Observation	$S^{95}_{\mathrm{obs.(exp.)}}$	$\langle \mathcal{A}\epsilon\sigma \rangle^{95}_{\mathrm{obs.(exp.)}}$ [fb]
hadron–hadron	3.1 ± 1.2	3	$5.5 \left(5.5^{+2.1}_{-1.3}\right)$	$0.27 \left(0.27^{+0.11}_{-0.06}\right)$
lepton–hadron (low-mass)	22.1 ± 4.7	20	$12.4 \left(13.2^{+4.9}_{-3.5}\right)$	$0.61 \left(0.65^{+0.24}_{-0.17}\right)$
lepton–hadron (high-mass)	2.1 ± 1.5	3	$6.4 \left(5.2^{+2.6}_{-0.9}\right)$	$0.31 \left(0.26^{+0.13}_{-0.04}\right)$

Exclusion limits are derived for the scalar top pair production, assuming $\tilde{t}_1$ decays with 100% branching ratio into $b\nu_\tau\tilde{\tau}_1$. The likelihood fit is performed with the expected signal and overall signal-strength parameter constraint to be positive. The control and signal region are fitted simultaneously, taking into account the experimental and theoretical systematic uncertainties as nuisance parameters. For each mass hypothesis, the expected limits are calculated for the hadron–hadron selection, the two lepton–hadron selections, and the statistical combination of the lepton–lepton selections described in Reference [4]. The selection giving the best expected sensitivity is used to compute the expected and observed CL_s value. The resulting exclusion contour is shown in Figure 4 demonstrating scalar top mass below
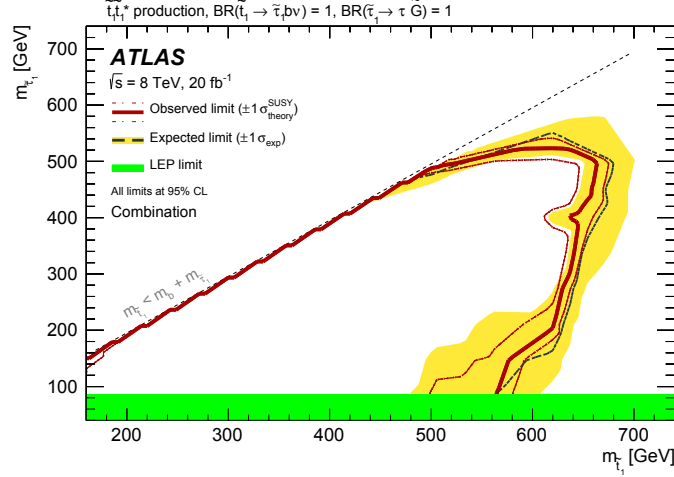
FIGURE 4. Observed and expected exclusion contours at 95% CL in the $(\tilde{t}_1, \tilde{\tau}_1)$ mass plane from the combination of all selections. The dashed and solid lines show the 95% CL expected and observed limits, respectively, including all uncertainties except for the theoretical signal cross-section uncertainty (PDF and scale). The band around the expected limit shows the $\pm 1\sigma$ expectation. The dotted $\pm 1\sigma$ lines around the observed limit represent the results obtained when varying the nominal signal cross section up or down by the theoretical uncertainty. The LEP limit on the mass of the scalar tau is also shown. Taken from Reference [3].

490 GeV to be excluded. Depending on the scalar tau mass, some models with scalar top masses up to 650 GeV are also excluded.

6   SUMMARY

A search for the direct pair production of supersymmetric partners of the top quark decaying via a scalar tau to lightest supersymmetric particle – nearly massless gravitino is performed. The data used in this analysis is collected in proton–proton collisions at center-of-mass energy, $\sqrt{s} = 8$ TeV, by the ATLAS detector during the 2012 operation of the LHC and corresponds to an integrated luminosity of 20 fb^{-1}. The scalar top candidates are searched for in events with either two hadronically decaying tau leptons, one hadronically decaying tau and one light lepton, or two light leptons. This is the first result from a hadron collider search for the three-body decay mode to scalar tau. Good agreement is observed between Standard Model background and the data, and lower limits on the scalar top mass are set at 95% confidence level. The lower limit on the scalar top mass is found to be between 490 GeV and 650 GeV for the scalar tau masses ranging from the LEP limit to scalar top mass.

7   ACKNOWLEDGMENTS

REFERENCES

[1]   R. Barbieri and G. F. Giudice, Nucl. Phys. **B306**, p. 63 (1988).
[2]   L. Evans and P. Bryant, JINST **3**, p. S08001 (2008).
[3]   ATLAS Collaboration, (2015), arXiv:1509.04976 [hep-ex] .
[4]   ATLAS Collaboration, JHEP **06**, p. 124 (2014), arXiv:1403.4853 [hep-ex] .
[5]   ATLAS Collaboration, Journal of Instrumentation **3**, p. S08003 (2008).
[6]   ATLAS Collaboration, Eur. Phys. J. **C72**, p. 1849 (2012), arXiv:1110.1530 [hep-ex] .
[7]   C. G. Lester and D. J. Summers, Phys. Lett. **B463**, 99–103 (1999), arXiv:hep-ph/9906349 [hep-ph] .
[8]   A. Barr, C. Lester, and P. Stephens, J. Phys. **G29**, 2343–2363 (2003), arXiv:hep-ph/0304226 [hep-ph] .
[9]   A. L. Read, Journal of Physics G: Nuclear and Particle Physics **28**, p. 2693 (2002).